Iran J Public Health, Vol. 52, No.3, Mar 2023, pp.563-574

Original Article

Serum Exosome-Derived MiR-7 Exacerbates Chronic Obstructive Pulmonary Disease by Regulating Macrophage Differentiation

Yiming Jiang, Jinhai Wang, He Zhang, Yeping Min, *Tijun Gu

Department of Emergency, The Affiliated Changzhou No.2 People's Hospital of Nanjing Medical University, Changzhou, 213003, China

***Corresponding Author:** Email: czpln102030@163.com

(Received 15 Aug 2022; accepted 19 Oct 2022)

Abstract

Background: Polarization of macrophages and miR-7 have been reported to greatly influence the progress of chronic obstructive pulmonary disease (COPD). However, the interaction is unclear. We aimed to investigate the role of miR-7 in the serum exosome of COPD, thus further revealing the underlying mechanism of COPD.

Methods: The study was conducted in 2022 in The Affiliated Changzhou No.2 People's Hospital of Nanjing Medical University, Changzhou, China. COPD mouse model was established. Macrophages were sorted by flow cytometry assay. ELISA kits were used to detect the levels of TNF-α and IL-6. Exosomes were identified by confocal microscopy and PKH67 staining. RT-qPCR and western blot assay were performed to determine the mRNA and protein expressions. H&E staining assay was used to assess the tissue injury. CCK-8 assay was applied to evaluate cell viability. Luciferase reporter assay was used to confirm the binding between PIM1 and miR-7.

Results: The exosomes derived from the COPD mice serum exerted high level of miR-7, which induced M1 differentiation of macrophages and increased the secretion of proinflammatory factors in vivo and in vitro. The effects of exosomes from COPD mice could be inhibited by miR-7 inhibitor. Bioinformatic prediction, luciferase reporter assay, and western blot assay showed an interaction between miR-7 and PIM1. Further examination showed that miR-7 regulated macrophage activation and differentiation to M1 via PIM1 in vitro.

Conclusions: miR-7 from serum exosomes might exacerbate COPD by stimulating macrophage differentiation to M1, supplying a potential therapeutic target for COPD treatment.

Keywords: Chronic obstructive pulmonary disease; Macrophage cells; M1 cells

Introduction

Chronic obstructive pulmonary disease (COPD) is a fatal disease with high mortality worldwide, accompanied with high health-care costs (1). It is characterized by progressively developed breathing obstruction, which is usually associated with lung inflammation caused by harmful particles or gases (2). Cigarette smoking (CS) is one of the most essential causes of COPD, which directly damages bronchial epithelial cells (BECs), the first barrier for respiratory tract, inducing excessive inflammation and ultimately leading to COPD (3). Although extensive researches have been conducted on the pathogenesis of COPD, there is still a lack of effective treatment options.

Copyright © 2023 Jiang et al. Published by Tehran University of Medical Sciences.
This work is licensed under a Creative Commons Attribution-NonCommercial 4.0 International license.
(https://creativecommons.org/licenses/by-nc/4.0/). Non-commercial uses of the work are permitted, provided the original work is properly cited

Patients with COPD still face with reduced life quality and even death threats (1).

Inhalation of harmful particles or gases usually induces inflammation in the lungs, which may lead to systemic inflammation and exacerbation of COPD (4). Macrophages are important effector cells in COPD by releasing pro-inflammatory cytokines, thereby regulating inflammation status in lung (5). Under stimulation, macrophages are differentiated into M1 or M2 types. M1 macrophages release many pro-inflammatory mediators, such as the inducible nitric oxide synthase (iNOS), interleukin 6 (IL-6), and the tumor necrosis factor-alpha (TNF-α), triggering inflammation in lungs (6). Conversely, M2 macrophages could enhance the expression of arginase-1 (Arg-1) to alleviate inflammatory responses (7). In the early phase of COPD, M1 macrophages are found to be increased in the bronchial submucosa of the patients (8), and continuous activation and polarization of macrophages to M1 phenotype aggravated COPD development (9). Therefore, the inhibition of the inflammation will benefit COPD recovery.

MicroRNAs (miRNAs) are ~20 nt small non-coding transcripts playing important regulatory roles in COPD (10). MiR-7 is one of the widely studied miRNAs, and it plays vital role in diverse human diseases. For instance, miR-7 was also reported to participate in the development of endocrine cells of pancreas (11) and neurons (12). miR-7 was significantly up-regulated in the serum of COPD patients, and was considered to be a biomarker for COPD (13). Exosomes, a type of extracellular vesicles with a diameter of 50-100 nm, are stable and serve as intercellular messengers by delivering small molecules among the cells. However, whether miR-7 exhibits regulatory function on COPD remains elusive.

We aimed to investigate the role of miR-7 in the serum exosome of COPD, thus further revealing the underlying mechanism of COPD.

Materials and Methods

Animals

The experiments were carried out in March 2022. Male C57BL/6 mice (6-8 weeks, 18-22g) were obtained from Nanjing University (Nanjing, China) and raised in a clean animal cabinet at 26 ℃, 12 h light/12 h dark period, with water and full nutrition food. After they acclimatized to the condition, ten mice were randomly selected and divided into control (n=5) and COPD (n=5) groups. COPD model was established as previous described (14). During animal experiment, the ARRIVE checklist was followed (15). In brief, mice from COPD or control group were placed in the glass chamber with holes of 2 cm diameters and exposed to cigarette smoke generated from Jiangjun cigarettes or not (tar ≤11 mg , nicotine ≤1.1 mg, CO ≤11 mg, Shandong China Tobacco Industry Co., Ltd.) for four hours per day for 28 days. At the end of modeling, lung function indexes of COPD model were determined, after which blood samples were obtained from the mice and the mice were sacrificed by cervical dislocation. For exosome treatment mice, mice in control-exosomes (n=5), and COPD-exosomes (n=5) groups were injected with serum-derived exosomes from control group or COPD group in the tail vein (20 μg of exosomes/mouse; exosomes were resuspended in 100 μl of PBS). Mice in the blank group (n=5) were injected with the same volume of PBS.

All animal experiments were approved by the Ethics Department of The Affiliated Changzhou No.2 People's Hospital of Nanjing Medical University (approval number: [2021]KY312-01).

Determination of the pulmonary functions

The pulmonary functions were assessed as previously described using Buxco system (16). Peek of inspiratory flow (PIF), peak of expiratory flow (PEF), and 50% tidal volume expiratory flow (EF50) were examined.

Purification of pulmonary macrophages

The macrophage cells were isolated from lungs as previously described (17). In brief, the lung tissues were minced and digested at 37°C for 0.5h, and centrifuged to remove the supernatant. Cells (2×10^8 cells/ml) were cultured, and macrophage

separation kit (Cat. TBD1092MAC, TBD, Tianjin, China) was used to isolate macrophages.

Cell culture and transfection

MH-S cells (ZQ0921) and 293T cells (ZQ0033) were obtained from Cell Research (China). MH-S cells were cultured in RPMI-1640 (Gibco, USA) with 10% FBS, 0.05mM β-Mer (Gibco, USA), and 1% PS. 293T cells were cultured in DMEM (high glucose, Gibco, USA) with 10% FBS (Gibco, USA) and 1% PS. Cells were maintained under 37 ℃ with 5% CO_2. For cell transfection, miR-7 mimic (5'- UGUUGUUUUAGUGAUCAGAAGGU-3'; 5'-ACCUUCUGAUCACUAAAACAACA-3'), miR-7 inhibitor (5'- ACCUUCUGAUCACUAAAACAACA-3'), si-PIM1 (5'-GATCATCAAGGGCCAAGTGTT-3'), and the related negative control were transfected using lipofectamine 3000 reagent (Ribobio, China) according to the manufacturer's illustration. Serumal exosomes (10 μg/ml) were incubated with cells for 36 h to examine the role of exosomes in macrophage polarization.

qRT-PCR

For lung-derived macrophages, exosomes, or cells, following the manufacturer's guidelines, total RNA was isolated by TRIzol reagent (Thermo Fisher Scientific, USA). PrimeScript miRNA cDNA Synthesis kit (cat. D350A, Takara Bio, Inc.) was used for reverse transcription. QPCR was then performed using SYBR Green reagent (SsoAdvanced Universal SYBR Green Supermix, cat. 1725274, Bio-Rad Laboratories, Inc.). U6 and GAPDH were miRNA and mRNA controls, respectively. $2^{-\Delta\Delta CT}$ method was employed to analyze the results (18). The primers are presented in Table 1.

Table 1: Primers used in this work

	Forward (5' – 3')	*Reverse (5' – 3')*
miR-7	GCGCGTGTTGTTTTAGTGATCA	AGTGCAGGGTCCGAGGTATT
PIM1	GATATTCCGTTTGAGCACG	AGGGACAGGCACCATTTA
iNOS	CCCTTCCGAAGTTTCTGGCAGCAGC	GGCTGTCAGAGAGCCTCGTGGCTTTGG
Arg-1	GGAAGCATCTCTGGCCACGCC	TCCCAGAGCTGGTTGTCAGGGG
U6	GCTTCGGCAGCACATATACTAAAAT	CGCTTCACGAATTTGCGTGTCAT
GAPDH	ACTCCACTCACGGCAAATTC	TCTCCATGGTGGTGAAGACA

Cell sorting by flow cytometry

F4/80, CD86, and CD206 were used as biomarkers for M0, M1, and M2 macrophage cells, respectively. MH-S cells under different treatments were labeled with flow cytometry antibodies targeting F4/80, CD86, and CD206 (Thermofisher, USA) following the guide protocol, and the cells were identified in flow cytometer (Thermofisher, USA) in APC, PE, and PE-CY7 channels, respectively. FlowJo software (Tree Star Inc., USA) was used for data analysis.

ELISA assay

After different treatments, serums or cell supernatants were collected and the total protein levels were determined by Bradford protein assay (Bio-Rad). According to the manufacturer's guidelines (R&D Systems), the levels of TNFα (MTA00B) and IL-6 (M6000B) in serums or cell supernatants were tested.

Exosome extraction, characterization, and analysis

Exosomes were isolated as previously described (19). In brief, serum was centrifuged to remove

cell debris and exosome pellets were resuspend using PBS. Exosomes were confirmed by electron microscopy and western blot. To determination whether exosomes could be taken up by recipients, the pellets were dyed with PKH67 (Beyotime, China) for 1 h at room temperature and nuclei were labeled with DAPI (Cat. No. D1306, Thermofisher, USA) for 6 h. Exosomes were visualized using confocal microscope (FV1000, Olympus, Japan) under 488 nm emission. For exosome treatment, 20 µg of exosomes isolated from serum were suspended in 100 µl of PBS and were injected into mice from tail vein.

Western blot

Proteins were extracted with RIPA buffer plus PMSF (Beyotime, China), separated by SDS-PAGE and transferred to PVDF. Primary antibodies used were CD81 (1:500, ab79559, Abcam), CD63 (1:500, ab134045, Abcam), PIM1 (1:500, ab54503, Abcam) or GAPDH (1:5000, ab8245, Abcam). Signals were detected using ECL detection system (GE Healthcare, Aurora, OH, USA). The intensities of the bands were analyzed by ImageJ 1.42q software (National Institutes of Health, Bethesda, MD, USA).

Pathological analysis and HE staining

HE staining were carried out as previously described (20) after heart perfusion was performed until the lung lobes turned white. Stained slices were analyzed using light microscope (Carl Zeiss, Jena, Germany).

Inflammation degrees and mean linear intercept (Lm) of the lung sections were assessed following the previous criterion (21). In brief, the severity of lung inflammation was scored from 0 to 3: 0, no inflammation; 1, mild inflammation; 2, moderate inflammation; 3, severe inflammation.

CCK-8 assay

Cells were seeded (100 µl/well) into a 96-well plate and were placed into the incubator 2 h (37°C, 5% CO_2). CCK-8 assay was performed according to the manufacturer's illustrations (ab228554, Abcam). The absorbance at 450 nm was determined.

Dual luciferase reporter assay

The putative binding site of PIM1 was cloned into the luciferase reporter vector as wild type 3'UTR of PIM1, while the binding site was mutated using the site-directed mutagenesis kit (NEB E0554, USA) and cloned into the vector as mutant type. PmiR-RB-REPORT vector (Ribobio, China) holding wildtype (WT) or mutant (MUT) 3'-UTR of PIM1 were transfected into 293T cells, together with miR-7 mimic, inhibitor or the associated controls using lipofectamine 3000 reagent (Invitrogen). After 48h, the luciferase activity was determined using a Dual-Luciferase Assay System (Promega, USA).

Statistical analysis

Statistical analysis was performed using GraphPad Prism 8.0 software (GraphPad Software, Inc.). Data are demonstrated as means ± standard deviation (SD). The normal distribution was estimated in GraphPad Prism 8.0 software before differential analysis. Two-tailed Student's t-test and one-way ANOVA with Turkey's post hoc test were performed to compare the difference among two or multiple groups, respectively. Data with *P* values smaller than 0.05 is considered significant. At least three independent replicates were carried out for each assay.

Results

The control group showed no histopathological signs of inflammation, which was contrary to the COPD group (Fig. 1A). Furthermore, inflammation score and Lm were both significantly enhanced in the COPD mice (Fig. 1B, P <0.0001; C, P<0.0001). Consistently, there were significant decreases in PIF, PEF, and EF50 in the COPD group (Fig.1D, PIF, P<0.0001; PEF P<0.0001; EF50, P<0.0001). The expression level of miR-7 in the serum showed an obvious enhancement in the COPD mice (Fig.1E, P <0.0001), and the similar change was observed in the macrophages from lung tissues (Fig. 1F, P= 0.0051). An increased number of macrophages was observed (Fig.1G). We also found an increased iNOS level

and a decreased Arg1 level, reflecting that macrophages were differentiated into M1 rather than M2 (Fig.1H; iNOS, *P*<0.0001; Arg1, *P*= 0.0007). In addition, the levels of the indicated pro-inflammatory cytokines secreted by macrophages were elevated significantly (Fig.1I; IL-6, *P*<0.0001; TNF-α, *P*<0.0001).

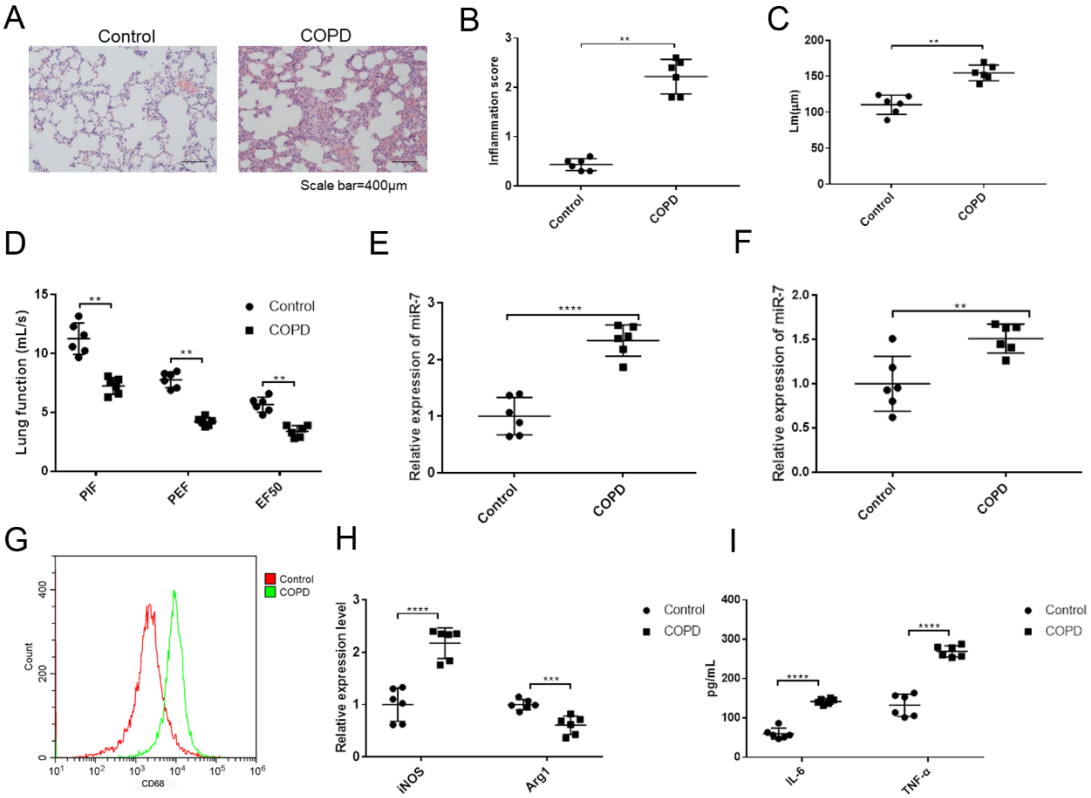

Fig. 1: The establishment and evaluation of the chronic obstructive pulmonary disease (COPD) model mice. A, HE staining of the lung tissues. B, Inflammation score and (C) the mean linear intercept (Lm) of the lung tissues. D, The peak inspiratory flow rate (PIF), peak respiratory flow rate (PEF), and 50% expiratory flow rate (EF50). E, The expression level of miR-7 by qRT-PCR in mice lungs. F, The expression level of miR-7 in macrophages. G, Macrophages in lung tissues were counted with flow cytometry. H, The expression level of iNOS and Arg-1 in mice lungs by qRT-PCR. I, ELISA assay for IL-6 and TNF-α in mice lungs under different treatment. * *P*<0.05 and ** *P*>0.01 vs. the control group

The effects of exosomes from COPD mouse serum on normal mouse

First, exosomes isolated from COPD mouse serum were identified under transmission electron microscope (TEM) (Fig. 2A). CD81, HSP70 and CD63, were positively expressed in exosomes, while Calnexin was not detected (Fig. 2B). MiR-7 was accumulated in the serum-derived exosomes form COPD group (Fig. 2C, *P*= 0.0014). COPD-exosomes caused inflammatory responses in lungs of normal mice but control-exosomes (Fig. 2D-F; E, *P* <0.0001; F, *P*<0.0001). The macrophages were accumulated in the stressed lung tissues and were differentiated into M1 type (Fig. 2G and H; H, iNOS, *P*<0.0001; H, Arg1, *P*= 0.00859); consequently, IL-6 and TNF-α were upregulated significantly (Fig. 2I, IL-6, *P*=0.006; TNF-α, *P*=0.0008). The mice under COPD-exo treatment also showed an increased miR-7 level (Fig. 2J, *P*= 0.006).

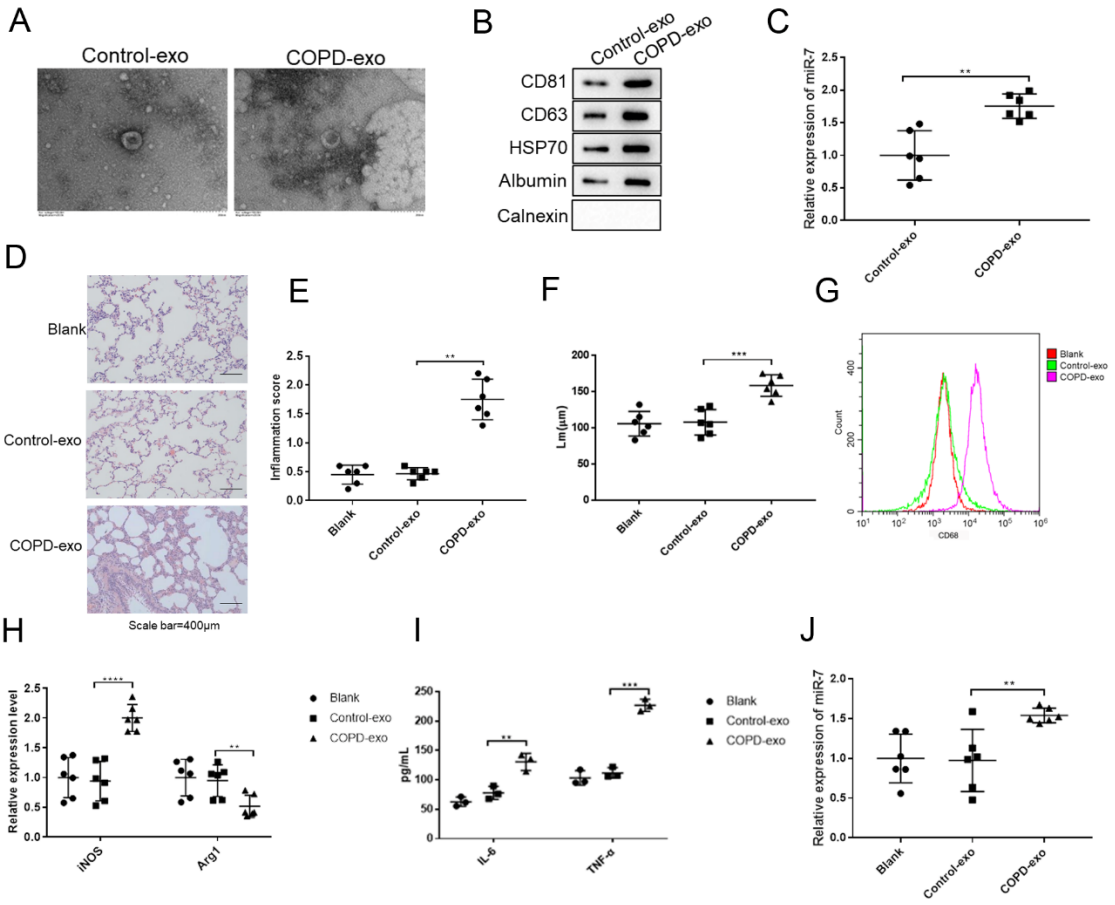

Fig. 2: The effects of COPD-serum derived exosomes on mice normal lung tissues. The exosomes isolated from mice serum were identified using transmission electron microscope (TEM) (A) and western blot (B). C, The expression levels of miR-7 in the exosomes. D, HE staining of lung tissues. E, The inflammation scores of lung tissues were assessed. F, the mean linear intercept (Lm) of the lung sections. G, The number of macrophage cells in lung tissues were detected with flow cytometry. H, The expression level of iNOS and Arg-1 in macrophages. I, ELISA assay for IL-6 and TNF-α. J, The expression level of miR-7 in macrophages. * P<0.05, ** P>0.01, and *** P>0.001 vs. the control/blank group

The effects of serum-derived exosomes on macrophage differentiation in vitro

PKH67-labeled exosomes could be up taken into the cytoplasm of macrophages (Fig. 3A). In the macrophages, the level of miR-7 in the COPD-exo group was significantly increased after co-cultured with COPD-exo (Fig. 3B, P<0.0001), which was in consistent with the results in vivo (Fig. 2H). COPD-exo notably enhanced the proliferation of macrophages than that of the control group (Fig. 3C, P<0.0001). Further, MH-S cells treated with the COPD-exosomes tended to polarize into M1 type rather than M2 type (Fig. 3D-G; E, P=0.0028; F, P=0.0037; G, P<0.0001). Significant increases of IL-6 and TNF-α could be detected in cells from COPD-exo group (Fig. 3H; IL-6, P=0.006; TNF-α, P=0.0003).

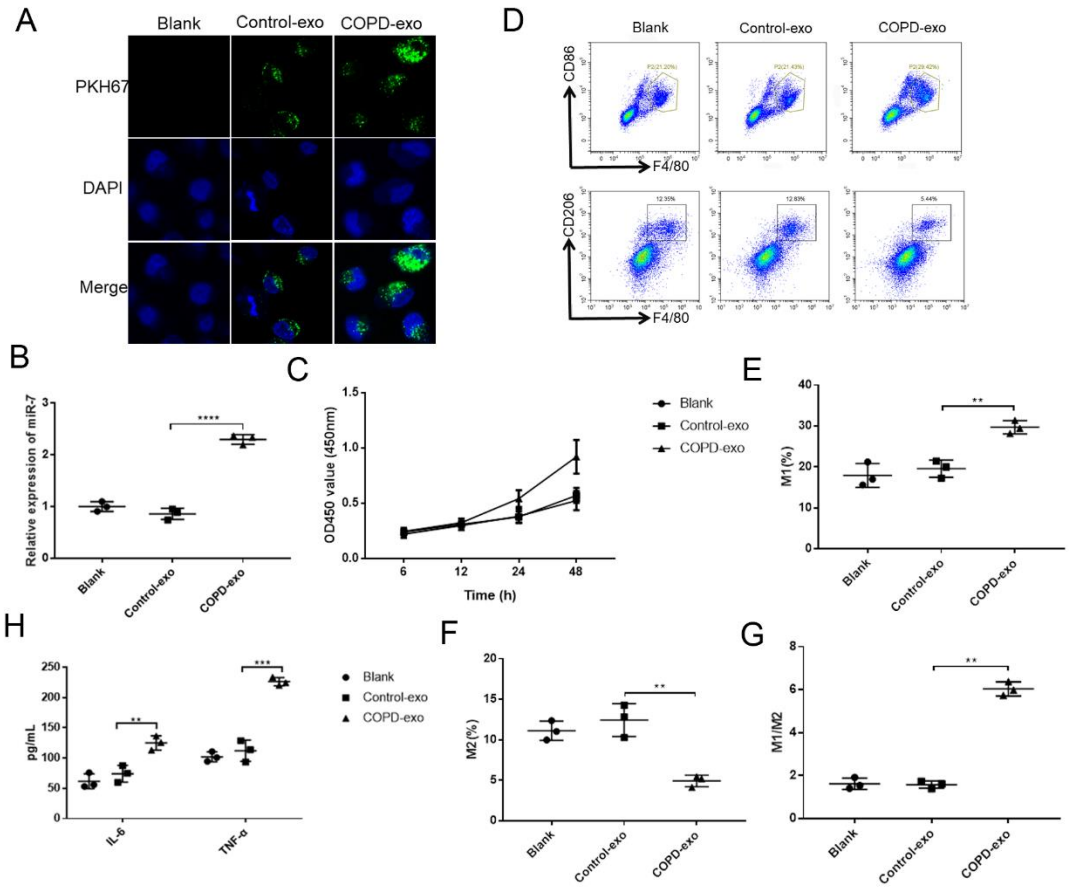

Fig. 3: The effects of COPD-serum derived exosomes on macrophage activation and polarization in vitro. A, Exosomes could be up-taken into MH-S cells. B, The expression levels of miR-7 in MH-S cells. C, Cell viability was determined by CCK-8 assay. The differentiation of the macrophages was determined by flow cytometry (D) and statistically analyzed (E-G). H, ELISA assay of IL-6 and TNF-α in the cells. Each assay was repeated for three times. * P<0.05, ** P>0.01, and *** P>0.001 vs. the control-exo group

The effect of miR-7 from serum-derived exosomes on macrophage activation and differentiation

Compared with the inhibitor NC group, miR-7 inhibitor decreased dramatically the level of miR-7, and impaired the cell proliferation triggered by COPD-exosomes (Fig. 4A, P<0.0001, NC inhibitor+COPD-exo vs. NC inhibitor; P=0.002, NC inhibitor vs. miR-7 inhibitor+COPD-exo; Fig. 4B P=0.00745, NC inhibitor+COPD-exo vs. NC inhibitor; P=0.04, NC inhibitor vs. miR-7 inhibitor+COPD-exo). Moreover, miR-7 inhibitor blocked M1 polarization of macrophages (Fig. 4C, P=0.003, NC inhibitor+COPD-exo vs. NC inhibitor; P= 0.01, miR-7 inhibitor+COPD-exo vs. NC inhibitor; Fig. 4D, P=0.001, NC inhibitor+COPD-exo vs. NC inhibitor; P= 0.004, miR-7 inhibitor+COPD-exo vs. NC inhibitor) and reduced the secretions of IL-6 and TNF-α (Fig. 4E, IL-6, P=0.0008, NC inhibitor+COPD-exo vs. NC inhibitor; P=0.005, NC inhibitor vs. miR-7 inhibitor+COPD-exo; TNF-α, P=0.003, NC inhibitor+COPD-exo vs. NC inhibitor; P=0.009, NC inhibitor vs. miR-7 inhibitor+COPD-exo), indicating an involvement of exosomal miR-7 in macrophage activation and differentiation.

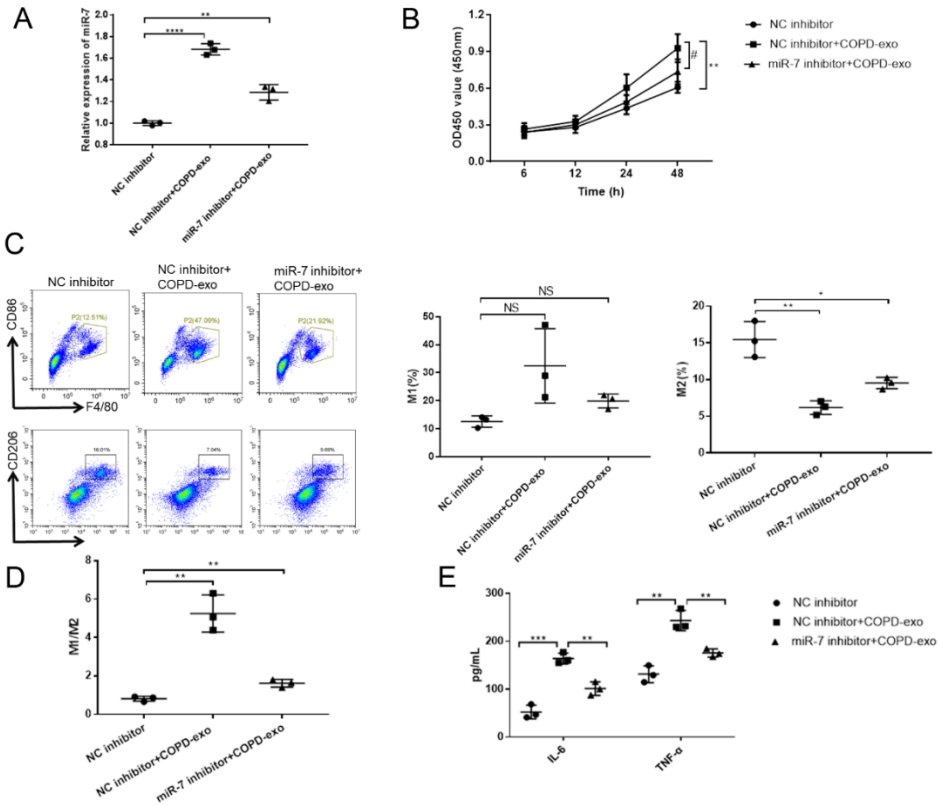

Fig. 4: The effects of exosomal miR-7 from COPD-mice on macrophage activation and polarization in vitro. A, The expression levels of miR-7 in MH-S cells. B, Cell viability was determined by CCK-8 assay. The differentiation of macrophages was determined by flow cytometry (C) and statistically analyzed (D). E, ELISA assay for IL-6 and TNF-α in the cells. Each assay was repeated for three times. * P<0.05, ** P>0.01, and *** P>0.001 vs. the NC inhibitor group. # P<0.05, ## P>0.01, and ### P>0.001 vs. the NC inhibitor+COPD-exo group

MiR-7 from serum-derived exosomes regulated PIM1

We then screened for the target gene of miR-7. Four miRNA databases (TargetScan, DIANA, miRwalk, and starBase), were used for miR-7 target prediction and 32 overlapping genes were shown in Fig. 5A. Based on our previous work and the published references, PIM1 was selected as a candidate target for miR-7. The putative binding sequences of PIM1 and miR-7 were listed in Fig. 5B (upper). The luciferase activity decreased significantly in cells co-transfected with miR-7 mimic and PIM1-WT (P=0.01), while miR-7 inhibitor produced the reverse results (P= 0.001). However, no significant change could be observed in PIM1-MUT group (Fig. 5B, lower). In COPD mice, PIM1 was downregulated in macrophages compared with the control group (Fig. 5C, P=0.007). In COPD-exosomes mice, both the expression and protein levels of PIM1 were decreased dramatically (Fig. 5D, P= 0.002; Fig. 5E, P= 0.003). Consistently, COPD-exosomes decreased the expression level and protein level of PIM1 in MH-S cells (Fig. 5F, P= 0.0005; Fig. 5G, P= 0.004), whereas miR-7 inhibitor could reverse the effects of COPD-exosomes (Fig. 5H, P=0.0003, NC inhibitor+COPD-exo vs. NC inhibitor; P=0.0008, NC inhibitor+COPD-exo vs. miR-7 inhibitor+COPD-exo; Fig. 5I, P=0.002, NC inhibitor+COPD-exo vs. NC inhibitor; P=0.003, NC inhibitor+COPD-exo vs. miR-7 inhibitor+COPD-exo), verifying that miR-7 could regulate PIM1 in vitro and in vivo.

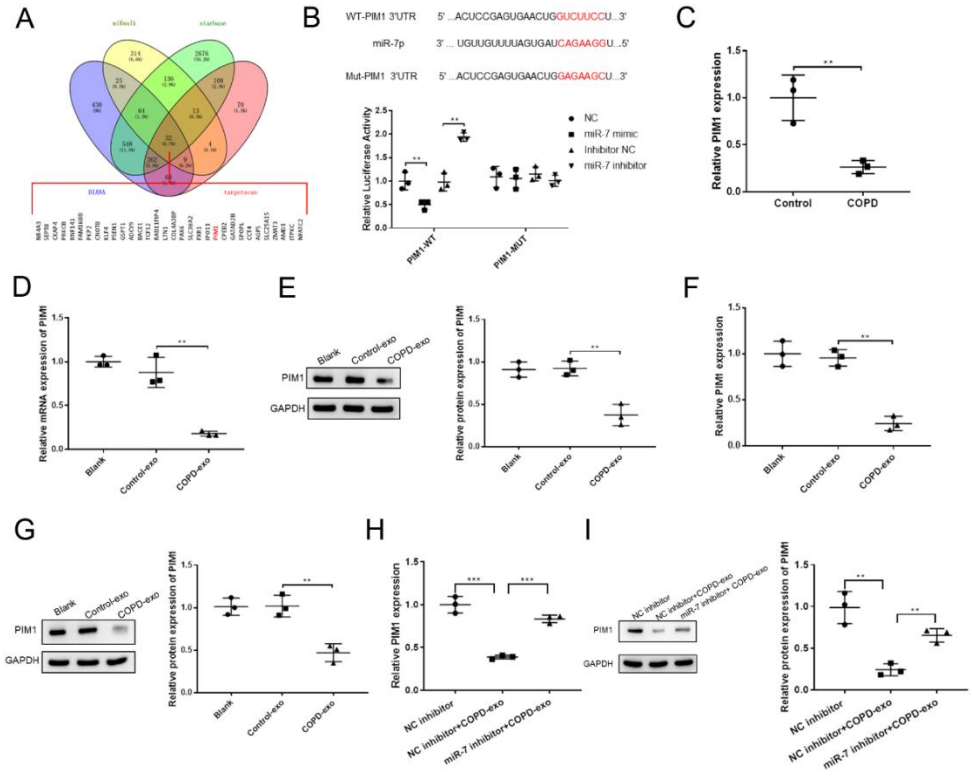

Fig. 5: The interaction of miR-7 and PIM1 in vitro and in vivo. A, The predicted potential targets of miR-7. B (upper), the binding sites of miR-7 and PIM1. B (lower), Luciferase activity of the transfected cells. C, The expression levels of PIM1 in macrophages from COPD mouse model. The expression levels (D) and protein levels (E) of PIM1 in COPD macrophages. The expression levels (F) and protein levels (G) of PIM1 in MH-S cells. The expression level (H) and protein level (I) of PIM1 in MH-S cells. H, The protein levels of PIM1 in MH-S cells. Each assay was repeated for three times. ** *P*>0.01, and *** *P*>0.001 vs. NC, inhibitor NC, control, or control-exo group

MiR-7 from serum-derived exosomes affected macrophage activation and differentiation via PIM1

MH-S cells co-cultured with COPD-exosomes were used for the following treatments. MH-S cells transfected with si-PIM1 displayed an obviously reduced PIM1 expression level (Fig. 6A, *P*=0.005). In addition, the silence of PIM1 could significantly reverse the inhibitory effect of miR-7 inhibitor on proliferation of macrophages (Fig. 6B, *P*=0.03, miR-7 inhibitor vs. NC inhibitor; *P*= 0.02, miR-7 inhibitor+si-NC vs. miR-7 inhibitor+si-PIM1). Moreover, the silence of PIM1 promoted macrophage polarization to M1 phenotype (Fig. 6C, M1: *P*= 0.007, miR-7 inhibitor vs. NC inhibitor; *P*=0.01, miR-7 inhibitor+si-NC vs. miR-7 inhibitor+si-PIM1; M2: *P*= 0.005, miR-7 inhibitor vs. NC inhibitor; *P*= 0.004, miR-7 inhibitor+si-NC vs. miR-7 inhibitor+si-PIM1; Fig. 6D, *P*= 0.003, miR-7 inhibitor vs. NC inhibitor; *P*= 0.008, miR-7 inhibitor+si-NC vs. miR-7 inhibitor+si-PIM1) and enhanced the secretions of IL-6 and TNF-α at the presence of miR-7 inhibitor (Fig. 6 E, IL-6: *P*= 0.0003, miR-7 inhibitor vs. NC inhibitor; *P*=0.007, miR-7 inhibitor+si-NC vs. miR-7 inhibitor+si-PIM1; TNF-α, *P*= 0.0007, miR-7 inhibitor vs. NC inhibitor; *P*=0.005, miR-7 inhibitor+si-NC vs. miR-7 inhibitor+si-PIM1), suggesting that miR-7 from serum-derived exosomes affected macrophage activation and differentiation by regulating PIM1.

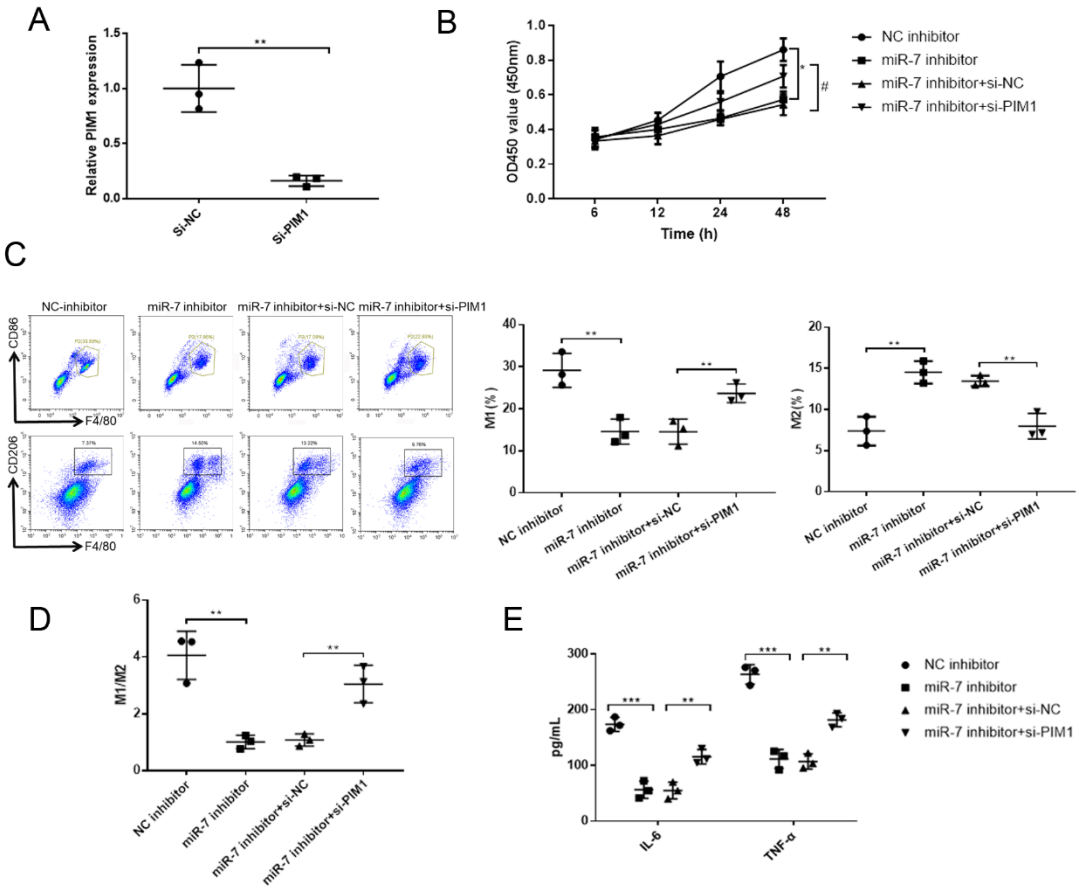

Fig. 6: The effects of miR-7 and PIM1 on macrophage activation and polarization. A, The expression level of PIM1 in the macrophages. B, Cell viability was determined by CCK-8 assay. The differentiation of the macrophages was determined by flow cytometry (C) and statistically analyzed (D). E, ELISA assay for IL-6 and TNF-α. Each assay was repeated for three times. * P<0.05, ** P>0.01, and *** P>0.001 vs. the NC inhibitor group. # P<0.05, ## P>0.01, and ### P>0.001 vs. miR-7 inhibitor + si-NC group

Discussion

In this work, we found a potential prognostic biomarker of COPD, that is, miR-7. Overexpressed miR-7 in the serum of the COPD mice aggravated COPD by enhancing M1 polarization of pulmonary macrophages, and PIM1 was the target gene of miR-7.

Phospholipid bilayer of exosomes could protect these small molecules from being degraded, so that the small molecules could serve as biomarkers for many diseases (22). Exosomes can be transferred to recipient cells to deliver small molecules and regulate the physiological metabolism of the recipient cells (23). Many miRNAs have been involved in the pathomechanism of COPD. For instance, miR-34a mediated the progression of female COPD under smoking exposure (24). In recent years, exosomal miRNAs in serum have attracted global attention for serving as reliable markers in liquid biopsy of COPD. Exosomes isolated from the cigarette smoke extract CSE-treated human bronchial epithelial cells caused myofibroblast differentiation phenotype of MRC-5 cells, attributed to miR-21 (25). Previously, miR-7 was obviously up-regulated in the

serum of COPD patients, which might be a powerful diagnostic biomarker for COPD (13). In emphysema, the methylation modification of miR-7 changed its anti-oncogenic role in lung cancer and promoted the development of emphysema (26). We found that miR-7 was notably enriched in COPD-exo, and exosomal miR-7 might be delivered to the alveolar macrophages, thus stimulating macrophage activation and M1 polarization to deteriorate COPD.

PIM1, a well-defined serine/threonine kinase, is involved in many cellular processes, including inflammation-related signal transduction (27). For example, PIM1 participated in airway inflammation in mice and the pro-inflammatory responses of fetal membranes (28). PIM1 protected cigarette smoke-treated mouse tracheal epithelial cells by reducing inflammation (29). Our work showed that miR-7 could downregulate the expression level of PIM1 in macrophage cells to stimulate macrophage M1 differentiation, enhancing the secretion of proinflammation factors, which might be responsible for the enhanced inflammation reaction and deteriorated COPD.

Conclusion

Serum exosomal miR-7 might exacerbate COPD by stimulating macrophage cell activation and M1 polarization through PIM1, supplying a potential therapeutic target for COPD treatment.

Journalism Ethics considerations

Ethical issues (Including plagiarism, informed consent, misconduct, data fabrication and/or falsification, double publication and/or submission, redundancy, etc.) have been completely observed by the authors.

Acknowledgements

No funding was received in this study.

Conflict of Interest

The authors declare that there is no conflict of interest.

References

1. López-Campos JL, Tan W, Soriano JB (2016). Global burden of COPD. *Respirology,* 21(1):14-23.
2. Pauwels RA, Rabe KF (2004). Burden and clinical features of chronic obstructive pulmonary disease (COPD). *Lancet,* 364(9434):613-20.
3. Zuo L, He F, Sergakis GG, et al (2014). Interrelated role of cigarette smoking, oxidative stress, and immune response in COPD and corresponding treatments. *Am J Physiol Lung Cell Mol Physiol,* 307(3):L205-18.
4. Agustí A, Edwards LD, Rennard SI, et al (2012). Persistent systemic inflammation is associated with poor clinical outcomes in COPD: a novel phenotype. *PLoS One,* 7(5):e37483.
5. Barnes PJ (2004). Alveolar macrophages in chronic obstructive pulmonary disease (COPD). *Cell Mol Biol (Noisy-le-grand),* 50 Online Pub:OL627-37.
6. Karadag F, Karul AB, Cildag O, Yilmaz M, Ozcan H (2008). Biomarkers of systemic inflammation in stable and exacerbation phases of COPD. *Lung,* 186(6):403-9.
7. Eapen MS, Hansbro PM, McAlinden K, et al (2017). Abnormal M1/M2 macrophage phenotype profiles in the small airway wall and lumen in smokers and chronic obstructive pulmonary disease (COPD). *Sci Rep,* 7(1):13392.
8. Saetta M, Baraldo S, Corbino L, et al (1999). CD8+ve cells in the lungs of smokers with chronic obstructive pulmonary disease. *Am J Respir Crit Care Med,* 160(2):711-7.
9. Hogg JC, Chu F, Utokaparch S, et al (2004). The nature of small-airway obstruction in chronic obstructive pulmonary disease. *N Engl J Med,* 350(26):2645-53.
10. Szymczak I, Wieczfinska J, Pawliczak R (2016). Molecular Background of miRNA Role in Asthma and COPD: An Updated Insight. *Biomed Res Int,* 2016:7802521.
11. Correa-Medina M, Bravo-Egana V, Rosero S, et

al (2009). MicroRNA miR-7 is preferentially expressed in endocrine cells of the developing and adult human pancreas. *Gene Expr Patterns,* 9(4):193-9.
12. Titze-de-Almeida R, Titze-de-Almeida SS (2018). miR-7 Replacement Therapy in Parkinson's Disease. *Curr Gene Ther,* 18(3):143-153.
13. Akbas F, Coskunpinar E, Aynaci E, Oltulu YM, Yildiz P (2012). Analysis of serum micro-RNAs as potential biomarker in chronic obstructive pulmonary disease. *Exp Lung Res,* 38(6):286-94.
14. Vlahos R, Bozinovski S, Gualano RC, Ernst M, Anderson GP (2006). Modelling COPD in mice. *Pulm Pharmacol Ther,* 19(1):12-7.
15. McGrath JC, Drummond GB, McLachlan EM, Kilkenny C, Wainwright CL (2010). Guidelines for reporting experiments involving animals: the ARRIVE guidelines. *Br J Pharmacol,* 160(7):1573-6.
16. Diaz EA, Chung Y, Lamoureux DP, et al (2013). Effects of fresh and aged traffic-related particles on breathing pattern, cellular responses, and oxidative stress. *Air Quality, Atmosphere and Health,* 6(2):431-444.
17. Canan CH, Gokhale NS, Carruthers B, et al (2014). Characterization of lung inflammation and its impact on macrophage function in aging. *J Leukoc Biol,* 96(3):473-80.
18. Livak KJ, Schmittgen TD (2001). Analysis of relative gene expression data using real-time quantitative PCR and the 2− ΔΔCT method. *Methods,* 25(4):402-408.
19. Tanaka Y, Kamohara H, Kinoshita K, et al (2013). Clinical impact of serum exosomal microRNA-21 as a clinical biomarker in human esophageal squamous cell carcinoma. *Cancer,* 119(6):1159-67.
20. Wu Y, Liu Y, Huang H, et al (2013). Dexmedetomidine inhibits inflammatory reaction in lung tissues of septic rats by suppressing TLR4/NF-κB pathway. *Mediators Inflamm,* 2013:562154.
21. Feng F, Jin Y, Duan L, et al (2016). Regulation of ozone-induced lung inflammation by the epidermal growth factor receptor in mice. *Environ Toxicol,* 31(12):2016-2027.
22. Santangelo A, Imbrucè P, Gardenghi B, et al (2018). A microRNA signature from serum exosomes of patients with glioma as complementary diagnostic biomarker. *J Neurooncol,* 136(1):51-62.
23. Madhavan B, Yue S, Galli U, et al (2015). Combined evaluation of a panel of protein and miRNA serum-exosome biomarkers for pancreatic cancer diagnosis increases sensitivity and specificity. *Int J Cancer,* 136(11):2616-27.
24. Velasco-Torres Y, Ruiz-López V, Pérez-Bautista O, et al (2019). miR-34a in serum is involved in mild-to-moderate COPD in women exposed to biomass smoke. *BMC Pulm Med,* 19(1):227.
25. Xu H, Ling M, Xue J, et al (2018). Exosomal microRNA-21 derived from bronchial epithelial cells is involved in aberrant epithelium-fibroblast cross-talk in COPD induced by cigarette smoking. *Theranostics,* 8(19):5419-5433.
26. Rosas-Alonso R, Galera R, Sánchez-Pascuala JJ, et al (2020). Hypermethylation of Anti-oncogenic MicroRNA 7 is Increased in Emphysema Patients. *Arch Bronconeumol (Engl Ed),* 56(8):506-513.
27. Santio NM, Koskinen PJ (2017). PIM kinases: From survival factors to regulators of cell motility. *Int J Biochem Cell Biol,* 93:74-85.
28. Wang J, Cao Y, Liu Y, Zhang X, Ji F, Li J, Zou Y (2019). PIM1 inhibitor SMI-4a attenuated lipopolysaccharide-induced acute lung injury through suppressing macrophage inflammatory responses via modulating p65 phosphorylation. *Int Immunopharmacol,* 73:568-574.
29. de Vries M, Heijink IH, Gras R, et al (2014). Pim1 kinase protects airway epithelial cells from cigarette smoke-induced damage and airway inflammation. *Am J Physiol Lung Cell Mol Physiol,* 307(3):L240-51.